Synergistic Effects of Electrical Stimulation and Aligned Nanofibrous Microenvironment on Growth Behavior of Mesenchymal Stem Cells

Lin Jin,†,‡ Bin Hu,‡ Zhanrong Li,† Jingguo Li,*,† Yanzheng Gao,† Zhenling Wang,*,‡ and Jianhua Hao*,§

† Henan Provincial People's Hospital, Zhengzhou University People's Hospital, Number 7 Weiwu Road, Zhengzhou 450003, P. R. China

‡ Henan Key Laboratory of Rare Earth Functional Materials, Zhoukou 466001, P. R. China

§ Department of Applied Physics, The Hong Kong Polytechnic University, Hong Kong, P. R. China

ABSTRACT: Incontrollable cellular growth behavior is a significant issue, which severely affects the functional tissue formation and cellular protein expression. Development of natural extracellular matrix (ECM) like biomaterials to present microenvironment cues for regulation of cell responses can effectively overcome this problem. The external simulation and topological characteristics as typical guiding cues are capable of providing diverse influences on cellular growth. Herein, we fabricated two-dimensional aligned conductive nanofibers (2D-ACNFs) by an electrospinning process and surface polymerization, and the obtained 2D-ACNFs provided the effects of both alignment and electrical stimulation (ES) on cellular response of human mesenchymal cells (hMSCs). The results of cellular responses implied that the obtained 2D-ACNFs could offer a synergistic effect of both ES and aligned nanopattern on

hMSC growth behavior. The effects could not only promote hMSCs to contact each other and maintain cellular activity but also provide positive promotion to regulate cellular proliferation. Thus, we believe that the obtained 2D-ACNFs will have a broad application in the biomedical field, such as cell culture with ES, directional induction for cell growth, and damaged tissue repair, etc. **KEYWORDS:** aligned nanofiber, cell culture, electrical stimulation, hMSCs, tissue engineering

1. INTRODUCTION

Tissue damage can significantly change the tissue function of the body, which leads to the disability of tissue and disturbs the quality of life quality for people.[1−4] A promising strategy for achieving tissue repair by human mesenchymal cells (hMSCs) combined with nanobiomaterials is a very effective technique in the biomedical area. In this process, the structure characteristics of biomaterials and contact cues are key elements. Previous studies indicated that suitable structure, conductive polymer, signaling pattern, and magnetic force could provide positive effects on hMSC proliferation and differentiation.[5−8] Therefore, the scaffold with ideal morphology and desired cues for regulating hMSC growth behavior could be able to regain the abilities of damaged tissue or achieve optimized tissue regeneration. Thus, there is a tremendous need to prepare scaffolds with functional features and optimized structure for providing a desired microenvironment for hMSC growth.

Extracellular matrix (ECM)-like nanofibrous scaffolds based on nanofibers make it easy to achieve controllability of structure and functionalization by changing

preparation conditions to meet complex tissue requirements.[9–16] However, there are still challenges in damaged or diseased tissue repair; for example, structure and contact cues cannot be able to effectively work in providing an optimum microenvironment for hMSC growth.[17–26] Therefore, some novel strategy should be used to develop an ideal nanofibrous scaffold offering various promising cues, such as alignment,[27–29] morphological characteristics,[30–32] surface functionalization,[33–36] ES,[37–39] and mechanical stimulation,[40] etc.

Although previous studies had some relevant investigations about the effects of the various cues on cellular growth behavior by a nanofibrous scaffold,[27,41–47] there is still not enough for a clear understanding of the synergistic action of various cues on biochemical response of hMSCs. As typical contact cues, physical stimulation and morphological characteristics are very crucial for regulating cellular growth behavior of hMSCs and controlling cellular function expression. Thus, it is very necessary to explore the influence of them on cellular growth behavior of hMSCs, thereby to meet complex requirements of implantable ECM in tissue engineering areas.

For the above purpose, we propose to investigate the role of aligned nanofibers combined with ES on cellular behavior of hMSCs. First, we fabricated 2D-ACNFs by our self-made electrospinning process and surface solvent dispersion polymerization. Second, we investigated the synergistic effect of alignment and electrical simulation on cellular response of hMSCs. The SEM images indicated that the as-prepared 2DACNFs have excellent alignment, uniform surface morphology, and desired diameter distribution. The electrochemical characterization also showed that the as-prepared 2D-

ACNFs have outstanding electrical property to offer ES for the cell culture system. In addition, the results of cellular response indicated that the obtained 2D-ACNFs could supply a comprehensive influence of both alignment and ES on hMSC growth behavior. In addition, we also observed that the synergistic effects of alignment combined with ES could remarkably promote hMSCs to contact each other, guide extension, and maintain cellular activity; moreover, these two factors also provided positive improvement to regulate cellular proliferation and adhesion. Thus, we believe that this new insight will have a great deal of application in the biomedical field, such as for cellular functional protein expression and damaged tissue repair, etc.

2. EXPERIMENTAL SECTION

2.1. Materials.

Poly(L-lactic acid) (PLLA, MW = 250k) was provided by Daigang Polymer (Jinan, China). N,N-Dimethylformamide (DMF) and dichloromethane (DCM) (A. R.) were obtained from Guangzhou Chemical Reagent Co. Conductive monomer 3,4-ethoxylene dioxy thiophene (EDOT) and ferric chloride were purchased from Sigma-Aldrich (China).

2.2. Fabrication of 2D-CANFs.

In this study, the PLLA 2D-ANFs were prepared by self-designed electrospun collector using our reported method.28 Subsequently, the obtained 2D-ANFs were used as a template to coat the conductive polymer layer (PEDOT layer) by interfacial polymerization in the EDOT, ferric chloride, and ethanol solution. After ethanol evaporation, a conductive PEDOT layer formed, and then the prepared 2D-CANFs

were treated using ethanol 3−5 times to remove residual chemicals. Finally, the 2D-CANFs were dried at room temperature for 24 h.

2.3. Structural and Chemical Characterization of 2D-ACNFs.

The morphology of 2D-ACNFs was examined using a Quanta 200 scanning electron microscope (SEM) analysis system (FEI, Netherlands). The chemical analysis was examined by Fourier transform infrared spectroscopy (FTIR, Nicolet 6700, Thermo Scientific, USA) and X-ray photoelectron spectroscopy (XPS).

2.4. Cell Culture and Characterization.

hMSCs were cultured on the 2D-ACNFs to evaluate response between cells and the nanofibers under ES, and 2D random conductive nanofibers (2DRCNFs) were set as control groups. First, the samples were tailored and sterilized in a 24-well tissue culture plate (TCP) as in a previously reported method,48−50 and then cells were cultured on the samples (cell density is 1.5 × 104 cells/well) after washing 3−5 times with PBS. The following step was to add DMEM medium (0.5 mL) including 10% FBS (v/v). These cell-conductive nanofiber constructs were incubated as hMSC-required conditions (humidified condition, 5% CO_2, 37 °C).

The effects of ES on hMSCs were performed to reveal a response between cells and the alignment of conductive nanofibers. Cells were seeded onto 2D-RCNFs and 2D-ACNFs after 24 h, and the stainless steel electrodes were added into the cell chambers and in close contact with the samples. Then, a pulsed electrical potential (100 Hz, 100 mV/ cm) was applied by electrodes (4 h of every day). For the cellular viability analysis, hMSCs were visualized after 7 days' culture on the 2D-ACNFs under ES.

After fixed by 3.0% paraformaldehyde for half of 1 h, the cytoskeleton of cells was stained by Phalloidin-FITC with a concentration of 5 μg/mL, and the nuclei of cells was stained by Hoechst 33258 with a concentration of 5 μg/ mL, respectively. Phalloidin-FITC and Hoechst 33258 were purchased from Sigma-Aldrich. Finally, these cellular constructs were imaged using laser scanning confocal microscopy (Leica Microsystem 2.60).

The response of cellular morphology on the 2D-RCNFs and 2DACNFs was measured using by SEM images. After 7 days' culture, the cell-conductive nanofiber constructs were fixed through 3.0% glutaraldehyde aqueous solution and then dehydrated using ethanol/ water (v/v) concentrations as reported methods. The samples were then dried for 24 h in flowing air and imaged after coating platinum/ palladium with a thickness of 10 nm.

The adhesion and proliferation of hMSCs on the 2D-ACNFs with/ without ES were measured at various culture time points as in our previously reported method.40 The fluorescent absorbance of the cell− nanofiber constructs was tested (485/535 nm) by a fluorescence plate reader (Victor3 multilabel, PerkinElmer, U.S.A.), and the number of cells was calculated using the absorbance standard of the known cell. Collagen expression of hMSCs cultured on 2D-ACNFs was measured as in a previously reported method.[51,52]

3. RESULTS AND DISCUSSION

3.1. Fabrication and Structure Characterization of 2DACNFs.

As the schematic diagram of preparation, three steps were involved in preparation

of 2D-ACNFs. First, 2D-ANFs as the template were prepared according to the previous work.[28] Briefly, the homemade electrospinning system with a rotating collector was used to fabricate 2D-ANFs. After 2 h electrospinning polymer solution on the special collector, the 2DANFs were obtained by removing nanofibers from aluminum foil (Figure 1).

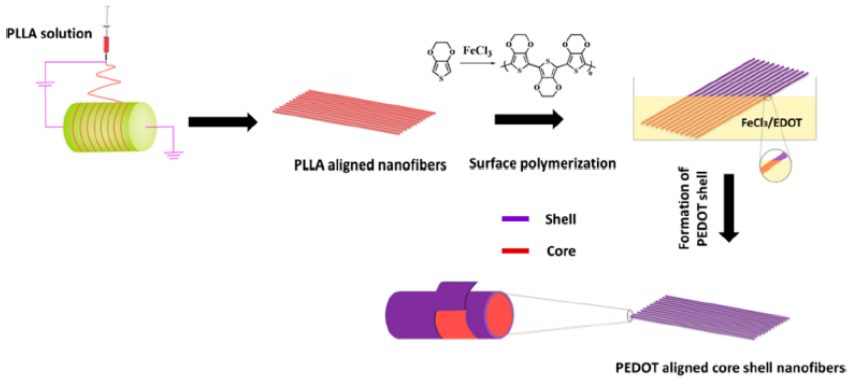

Figure 1. Schematic diagram of the 2D-ACNF fabrication process by an improved electrospinning process combined with EDOT surface polymerization.

The morphology of the obtained 2D-ANFs showed excellent alignment (Figure 2C); the majority of the nanofibers in the 2D-ANFs goes along the same direction (Figure S1); and the nanofiber with deviation degree less than 10° was up to 70% . The compactness of the obtained 2D-ANFs was much higher compared to 2D-RNFs (Figure 2A). The diameter of the nanofibers in the 2D-ANFs ranged from 380 to 560 nm, and the average diameter was 470 nm. Subsequently, the obtained 2D-ANFs were immersed into an EDOT/FeCl3 solution. Lastly, the conductive polymer PEDOT was coated on the nanofiber surface of the obtained 2D-ANFs after polymerization by solvent evaporation method (the schematic diagram of polymerization was shown in Figure 1). The structure of the obtained 2D-ACNFs was shown in Figure 2D and

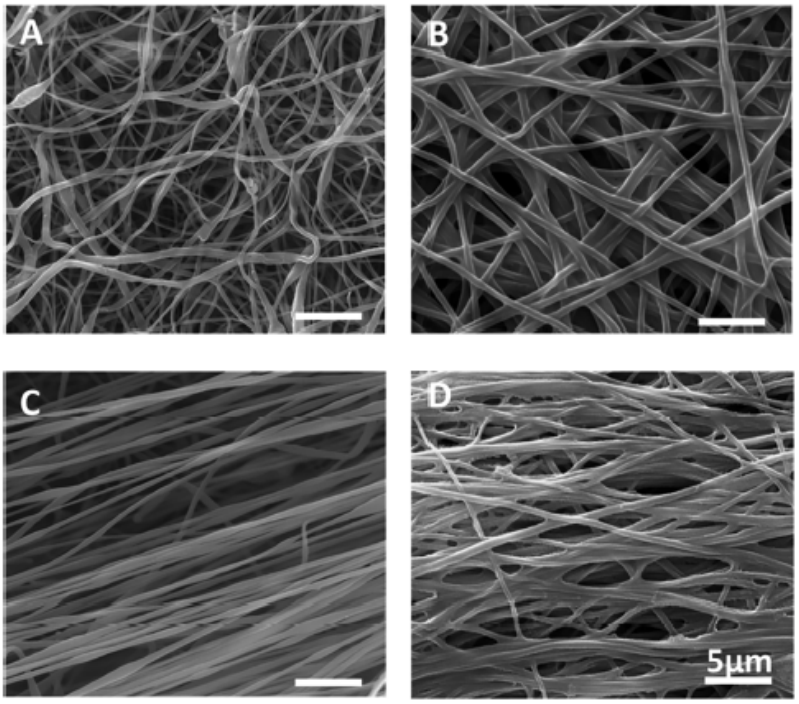

Figure 2. SEM images of (A) 2D-RNFs, (B) 2D-RCNFs, (C) 2D-ANFs, and (D) 2D-ACNFs.

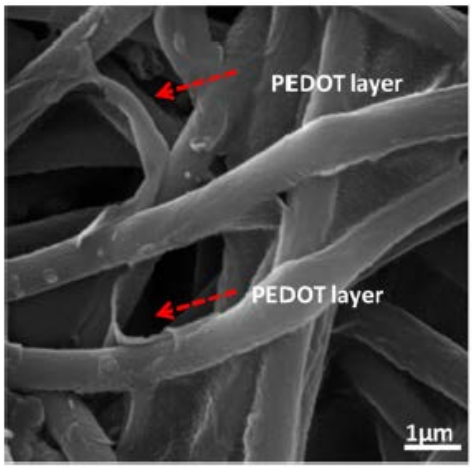

Figure 3. High-magnification SEM image of 2D-ACNFs. The average dimeter was 950 ± 100 nm.

Figure 3. The results indicated that the core−shell structure was successfully formed by surface polymerization, and the average diameter of the conductive nanofibers was 950 ± 100 nm. The FTIR results of 2D-ACNFs were shown in Figure 4A, which clearly demonstrated that the characteristic peaks of PEDOT were observed. The peaks of 1208 and 1095 cm−1 were the symmetric and asymmetric C−O−C stretching; the peak of

1445 cm−1 was the C☐C stretching of the thiophene ring; and the peaks of 9706, 845, and 705 cm−1 were characteristic absorption of C−S. The EDS mapping indicated that the characteristic peak of the S element on the surface of nanofibers in the PEDOT was also observed (Figure 5). These results noted that the PEDOT layer was successfully coated on the surface of aligned PLLA nanofibers.

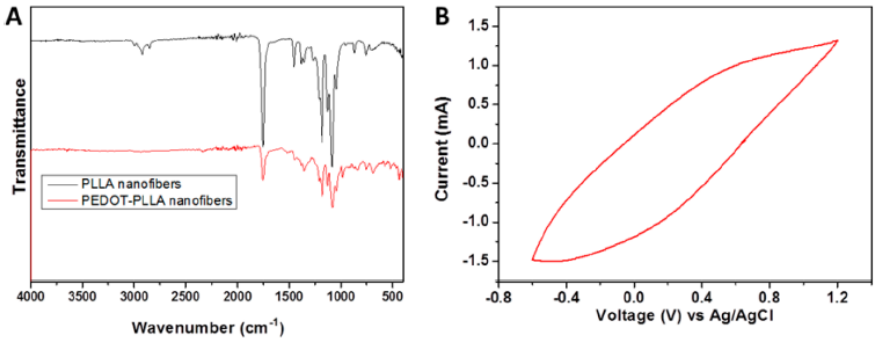

Figure 4. (A) FTIR spectra of raw nanofibers and 2D-ACNFs. (B) CV curve of 2D-ACNFs.

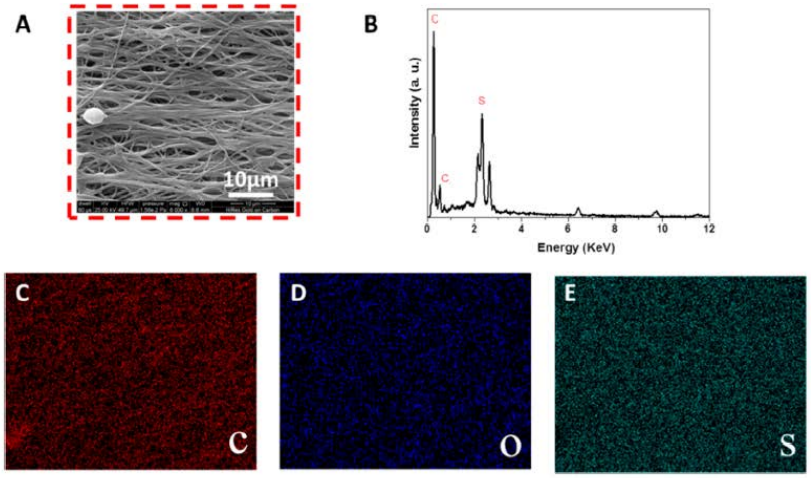

Figure 5. (A) SEM image of 2D-ACNFs. (B) EDS of the obtained 2D-ACNFs. The corresponding EDS mapping of elements (C) C, (D) O, and (E) S.

The electrical property of 2D-ACNFs was measured using the 2D-ACNFs as a working electrode according to a previous method.28 The result of electrochemical performance indicated that 2D-ACNFs have a high charge storage capacity under a scan rate of 25 mV/s (Figure 4B), which also showed that 2DACNFs as a cell culture substrate could provide appropriate current for cellular ES.

3.3. Cellular Response of hMSCs on the 2D-ACNFs.

Previous reports indicated that ES or alignment has a great effect on cellular growth behavior.[19,20] To reveal the synergistic effects from ES and alignment on cellular response, hMSCs as a cell model were used to evaluate the effect of alignment and electrical simulation on cells. hMSCs were cultured on the 2DACNFs and 2D-RCNFs with pulsed ES every day during the incubation period. The schematic diagram of ES for hMSCs was shown in Figure 6. After 7 days' culture, the cytoskeletal Factin of hMSCs displayed obvious differences on the various substrates.

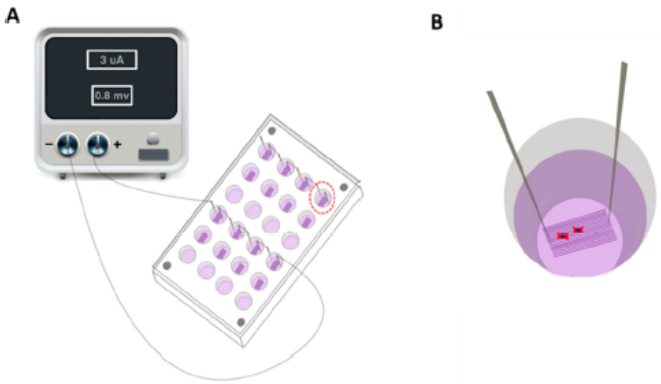

Figure 6. (A) Schematic illustration of cell cultures on the 2D-ACNFs with electrical stimulation environment. (B) The magnified illustration of a single well in electrical stimulation conditions.

As shown in fluorescent images (stained by halloidin-FITC and Hoechst 33258, respectively), hMSCs cultured on the raw random nanofibers showed a separate shape and had a sparse contact among cells, and the cytoskeleton could not fully expand (Figure 7A1−3). While cells on the conductive nanofibers of 2D-RCNFs showed good expansion, the shape of these cells demonstrated well-developed cellular nanofiber constructs along the separate conductive nanofibers (Figure 7B1−3). However, under pulsed ES environment, hMSCs cultured on the 2D-RCNFs showed much better extension than that without ES (Figure 7C1−3). In addition, the morphology of hMSCs

after 7 days' culture on the different substrates also demonstrated a similar phenomenon as fluorescent images. Figure 7A4 shows the morphology of hMSCs on the raw PLLA nanofibers, and these cells adhered on the PLLA nanofibers tightly and displayed round shape. The cells cultured on the 2D-RCNFs showed a relatively poor state due to the PEDOT layer coated on the surface of nanofibers that reduced the substrate's biocompatibility (Figure 7B4), which was disadvantageous for hMSC growth and contact. In contrast, cellular viability and morphology of cells cultured on the 2D-RCNFs with a pulsed ES (Figure 7C4) demonstrated significantly better than that without ES. These results indicated that the morphological characteristics were in agreement with features of the fluorescent images.

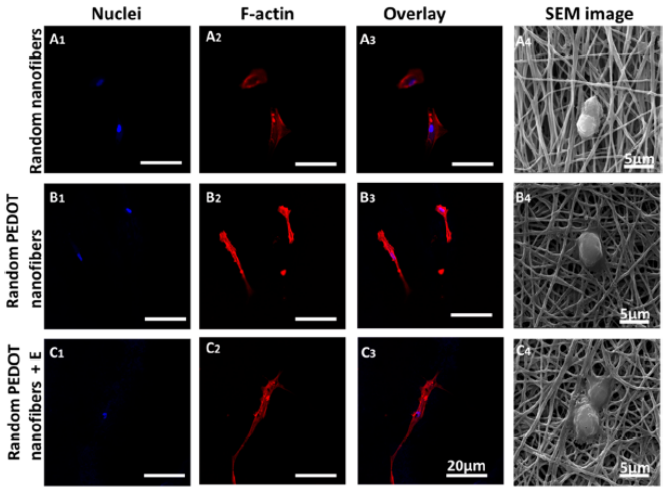

Figure 7. (A_{1-3}–C_{1-3}) Fluorescence and (A_4–C_4) SEM images of hMSCs cultured on 2D random nanofibers before and after coating conductive polymer after 7 days cultured with/without ES.

ES can supply physical stimulations for cells to regulate cellular proliferation, differentiation, and functional protein expression. To evaluate relevant biochemical changes, the proliferation and collagen expression of hMSCs were measured (Figure 8), and the results demonstrated that proliferation of hMSCs cultured with ES were slightly higher compared to that without ES during the 7 day culture period (Figure 8A).

However, the collagen expression of hMSCs with ES was not significantly different from that of cells without ES, while both of them were much more than that on the raw PLLA nanofibers. In addition, from Figure 8 B, we found that the collagen expression cultured on the conductive with/without ES was much higher than that on the raw PLLA nanofibers. These results showed that the cellular proliferation of hMSCs had no great influence with/without the daily pulsed ES, while conductive substrates could improve the collagen expression.

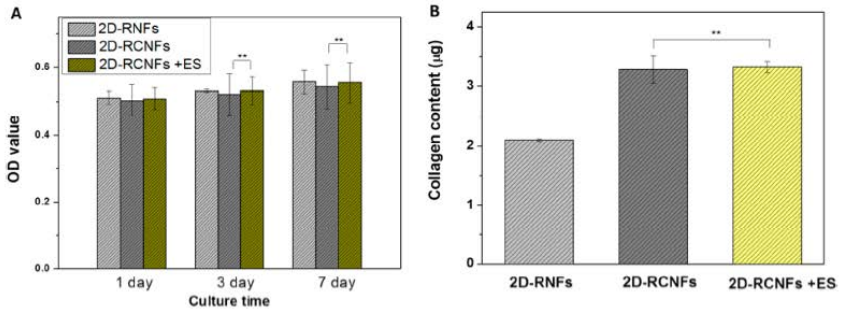

Figure 8. (A) Proliferation and (B) collagen expression of hMSCs cultured on 2D random nanofibers before and after coating conductive polymer after 7 days cultured with/without ES. Data are mean SD, $n = 4$, $^{*}P < 0.05$, $^{**}P < 0.01$.

To further explore the effect of alignment and ES on cellular behavior, hMSCs were cultured on the 2D-ACNFs for evaluating the response of cells. As shown in Figure 9C4, hMSCs displayed good extension; more interestingly, the signs of cell migration showed that cells displayed more obvious formation of connection area compared to that on the 2DRCNFs, and the connection was perpendicular to those aligned conductive nanofibers under ES. Moreover, the fluorescence images of hMSCs cultured on the 2D-ACNFs demonstrated that cytoskeletal F-actin of hMSCs could also connect each other or have a tendency for connection and then form a simple tissue-like type (Figure 9C1−3).

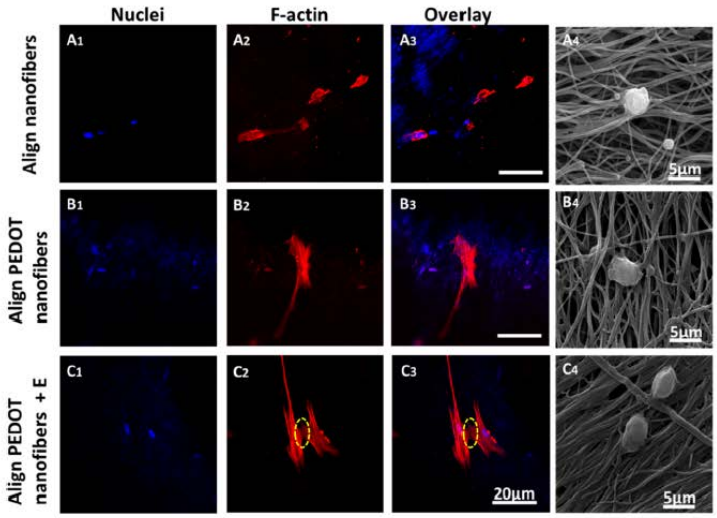

Figure 9. (A_{1-3}–C_{1-3}) Fluorescence and (A_4–C_4) SEM images of hMSCs cultured on 2D aligned nanofibers before and after coating conductive polymer after 7 days cultured with/without electrical stimulation.

hMSCs cultured on the 2D-ACNFs without ES also displayed spread, but the activity of the cell had slightly worse trend compared to that under ES (Figure 9B1−3). In contrast, hMSCs on raw aligned nanofibers contracted tightly, and the cells could be able to display directional growth (Figure 9A1−3). These results demonstrated that the synergistic effect of alignment and ES could promote hMSCs to contact each other, thus improving the formation of tissue. In addition, the morphology of cells was characterized for assessment of cellular response. As shown in Figure 9C4, the morphological characteristics of cells cultured on the 2D-ACNFs with ES displayed that cellular pseudopods connected to each other, while cells that were cultured without ES showed good spread and tightly adhered on the surface of the 2D-ACNFs (Figure 9B4). Moreover, we also found that these cells were slightly more contracted than that with ES, which might be attributed to the effect of the PEDOT layer. In addition, the cells cultured on raw aligned nanofibers were tightly adhered on the surface of the nanofibers (Figure 9A4). These morphological characteristics combined with fluorescent images demonstrated that the synergistic effects of ES and alignment could

enhance and maintain a positive promotion for cellular activity and growth. The results also indicated that the interaction of the two factors might be beneficial to promote the development of the hMSCs to the tissue-like formation.

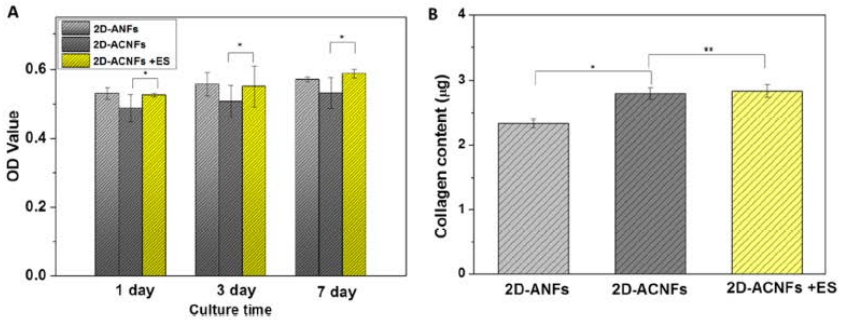

Figure 10. (A) Proliferation and (B) collagen expression of hMSCs cultured on 2D aligned nanofibers before and after coating conductive polymer after 7 day culture with/without ES. Data are mean SD, $n = 4$, $^{*}P < 0.05$, $^{**}P < 0.01$.

To investigate the impact of alignment and ES of nanofibers on biochemical functions, the proliferation and collagen expression of hMSCs cultured on 2D ACNFs were measured (Figure 10), and the test results indicated that the proliferation of hMSCs cultured with ES was much higher compared to that without ES during the 7 day culture period (Figure 10A). Moreover, the collagen expression of hMSCs cultured on conductive substrates was significantly more than that on the aligned PLLA nanofibers, and ES has no significant influence on collagen expression (Figure 10B). These results showed that the synergistic effect of alignment and ES can improve proliferation of hMSCs, meanwhile, which also showed daily pulsed ES had no great influence on collagen expression.

The obtained results indicated that the geometry cues of 2DACNFs displayed close morphological resemblance of the nanofibrous microenvironment to hMSCs and could demonstrate a good biocompatibility and promote cellular growth and some protein expression, but no obvious migration was achieved.[6,53] Providing ES cues for hMSCs

by 2D-ACNFs, the significant promotion was observed, which might be attributed to the influx of Ca^{2+} induced by the depolarizing current. These Ca^{2+} further activated the calmodulin-kinases to elicit hMSC outgrowth and expedite hMSC migration. Compared to the effect of a traditional single physical cue, this new strategy for cellular ES with the alignment of 2DACNFs will supply more controllable parameters and the possibility for the regeneration and repair of damaged or have a broad application in the tissue engineering field.

The obtained results were consistent with previous studies,[6,10,53] without ES, and the geometry cues of 2DACNFs displayed close morphological resemblance of the nanofibrous microenvironment to hMSCs[17] and could demonstrate a good biocompatibility and promote cellular growth and some protein expression; however, no obvious migration was achieved. The interaction between the hMSCs and the nanofibers of 2D-ACNFs was much stronger compared to the interaction between hMSCs and the nanofibers of 2DRCNFs (Figure 7B4, Figure 9B4). In contrast, under the ES microenvironment, the significant phenomenon was observed, and the hMSCs displayed much more pronounced trend for switching to perpendicular outgrowth along the nanofibers of 2D-ACNFs (Figure 7C4, Figure 9C4), which might be attributed to the influx of Ca^{2+} induced by the depolarizing current. These Ca^{2+} further activated the calmodulin-kinases to elicit hMSC outgrowth and expedite hMSC migration and growth. Compared to the effect of a traditional single physical cue, this new strategy for cellular ES with the alignment of 2DACNFs will supply more controllable parameters and the possibility for the regeneration and repair of damaged or diseased

tissue.[54] It is expected that the obtained 2D-ACNFs will have a broad application in the tissue engineering field.

4. CONCLUSION

In conclusion, we successfully fabricated 2D-ACNFs by the electrospinning process and surface polymerization. The asprepared 2D-ACNFs exhibited excellent alignment, electrical property, and biocompatibility. In addition, we had a detailed investigation on the effects of alignment and electrical simulation on the cellular response of hMSCs. The gained cellular response results indicated that the obtained 2D-ACNFs could offer two aspects to mainly influence hMSC growth behavior. First, the synergistic effect of alignment combined with ES could promote hMSCs to contact each other and maintain cellular activity, and second, these two factors also provided positive promotion to regulate cellular proliferation but had no great advantage in collagen expression. The synergistic effects of D-ACNFs also improve the tissue-like formation, which is important for regeneration and repair of damaged tissue. Thus, it is expected that the obtianed 2DACNFs will have a broad application in the biomedical field, such as cell culture with ES, directional induction for cell growth, and damaged tissue repair, etc.

AUTHOR INFORMATION

Corresponding Authors *E-mail: lijingguo@zzu.edu.cn (J.L.). *E-mail: zlwang2007@hotmail.com. Fax: (86)394-8178518. Tel.: (86)394-8178518 (Z.L.W.). *E-mail: jh.hao@polyu.edu.hk (J.H.).

The authors declare no competing financial interest.

ACKNOWLEDGMENTS

This research was supported by the National Natural Science Foundation of China (the number of funding is 51572303, 21504082, and 81600775) and the program of Innovative Talent (in Science and Technology) in University of Henan Province (the number of funding is 17HASTIT007). B. Hu acknowledges the Henan Natural Science Foundation (182300410204).

REFERENCES

(1) Shi, W. L.; Sun, M. Y.; Hu, X. Q.; Ren, B.; Cheng, J.; Li, C. X.; Duan, X. N.; Fu, X.; Zhang, J. Y.; Chen, H. F.; Ao, Y. F. Structurally and Functionally Optimized Silk-Fibroin−Gelatin Scaffold Using 3D Printing to Repair Cartilage Injury In Vitro and In Vivo. Adv. Mater. 2017, 29, 1701089.

(2) Walczak, E. M.; Hammer, G. D. Regulation of the Adrenocortical Stem Cell Niche: Implications for Disease. Nat. Rev. Endocrinol. 2015, 11, 14−28.

(3) Lutolf, M. P.; Gilbert, P. M.; Blau, H. M. Designing Materials to Direct Stem-Cell Fate. Nature 2009, 462, 433−441.

(4) Pera, M. F.; Tam, P. P. L. Extrinsic Regulation of Pluripotent Stem Cells. Nature 2010, 465, 713−720.

(5) Jin, L.; Xu, Q. W.; Kuddannaya, S.; Li, C.; Zhang, Y. L.; Wang, Z. L. Fabrication and Characterization of Three Dimensional Core-Shell Structure Nanofibers Designed for 3D Dynamic Cell Culture. ACS Appl. Mater. Interfaces 2017, 10, 17718−17726. (6) Jin, L.; Xu, Q. W.; Wu, S. Y.; Kuddannaya, S.; Li, C.; Huang, J. B.; Zhang, Y. L.; Wang, Z. L. Synergistic Effects of Conductive ThreeDimensional Nanofibrous

Microenvironments and Electrical Stimulation on the Viability and Proliferation of Mesenchymal Stem Cells. ACS Biomater. Sci. Eng. 2016, 2, 2042−2049.

(7) Chrzanowski, W.; Lee, J. H.; Kondyurin, A.; Lord, M. S.; Jang, J. H.; Kim, H. W.; Bilek, M. M. M. Nano-Bio-Chemical Braille for Cells: The Regulation of Stem Cell Responses using Bi-Functional Surfaces. Adv. Funct. Mater. 2015, 25, 193−205.

(8) Fayol, D.; Frasca, G.; Le Visage, C.; Gazeau, F.; Luciani, N.; Wilhelm, C. Use of Magnetic Forces to Promote Stem Cell Aggregation During Differentiation, and Cartilage Tissue Modeling. Adv. Mater. 2013, 25, 2611−2616.

(9) Selvaraj, S.; Fathima, N. N. Fenugreek Incorporated Silk Fibroin Nanofibers -A Potential Antioxidant Scaffold for Enhanced Wound Healing. ACS Appl. Mater. Interfaces 2017, 9, 5916−5926.

(10) Richards, D. J.; Tan, Y.; Coyle, R.; Li, Y.; Xu, R. Y.; Yeung, N.; Parker, A.; Menick, D. R.; Tian, B. Z.; Mei, Y. Nanowires and Electrical Stimulation Synergistically Improve Functions of hiPSC Cardiac Spheroids. Nano Lett. 2016, 16, 4670−4678.

(11) Wu, T.; Li, D. D.; Wang, Y. F.; Sun, B. B.; Li, D. W.; Morsi, Y.; El-Hamshary, H. E.; Al-Deyab, S. S.; Mo, X. M. Laminin-Coated Nerve Guidance Conduits Based on Poly(L-lactide-co-glycolide) Fibers and Yarns for Promoting Schwann Cells' Proliferation and Migration. J. Mater. Chem. B 2017, 5, 3186−3194.

(12) Sun, B. B.; Wu, T.; Wang, J.; Li, D. W.; Wang, J.; Gao, Q.; Bhutto, M. A.; El-Hamshary, H.; Al-Deyab, S. S.; Mo, X. M. Polypyrrole-Coated Poly(L-lactic acid-co-ecaprolactone)/Silk Fibroin Nanofibrous Membranes Promoting Neural Cell Proliferation and Differentiation with Electrical Stimulation. J. Mater. Chem. B 2016,

4, 6670−6679.

(13) Zhang, M. F.; Zhao, X. N.; Zhang, G. H.; Wei, G.; Su, Z. Q. Electrospinning Design of Functional Nanostructures for Biosensor Applications. J. Mater. Chem. B 2017, 5, 1699−1711.

(14) Xu, Y.; Cui, W. G.; Zhang, Y. X.; Zhou, P. H.; Gu, Y.; Shen, X. F.; Li, B.; Chen, L. Hierarchical Micro/Nanofibrous Bioscaffolds for Structural Tissue Regeneration. Adv. Healthcare Mater. 2017, 6, 1601457.

(15) Xing, Q.; Qian, Z. C.; Tahtinen, M.; Yap, A. H.; Yates, K.; Zhao, F. Aligned Nanofibrous Cell-Derived Extracellular Matrix for Anisotropic Vascular Graft Construction. Adv. Healthcare Mater. 2017, 6, 1601333.

(16) Allison, S.; Ahumada, M.; Andronic, C.; McNeill, B.; Variola, F.; Griffith; Ruel, M.; Hamel, V.; Liang, W. B.; Suuronen, E. J.; Alarcon, E. I. Electroconductive Nanoengineered Biomimetic Hybrid Fibers for Cardiac Tissue Engineering. J. Mater. Chem. B 2017, 5, 2402−2406.

(17) Liu, K.; Wang, N.; Wang, W. S.; Shi, L. X.; Li, H.; Guo, F. Y.; Zhang, L. H.; Kong, L.; Wang, S. T.; Zhao, Y. A Bio-Inspired High Strength Three-Layer Nanofiber Vascular Graft with Structure Guided Cell Growth. J. Mater. Chem. B 2017, 5, 3758. (18) Jin, L.; Wang, T.; Feng, Z. Q.; Leach, M. K.; Wu, J. H.; Mo, S. J.; Jiang, Q. A facile approach for the fabrication of core-shell PEDOT nanofiber mats with superior mechanical properties and biocompatibility. J. Mater. Chem. B 2013, 1, 1818−1825. (19) Jin, L.; Wang, T.; Zhu, M. L.; Leach, M. K.; Naim, Y. I.; Corey, J. M.; Feng, Z. Q.; et al. Electrospun Fiber and Tissue Engineering. J. Biomed. Nanotechnol. 2012, 8, 1−9.

(20) Wang, T.; Yuan, J. X.; Jin, L.; Feng, Z. Q.; Wu, J. H.; Zheng, J.; Wang, H. Y.; Xu, Z. W.; Guo, L. L.; He, N. Y. Fabrication and Characterization of Heparin Grafted Poly-L-lactic acid-Chitosan CoreShell Nanofibers Scaffold for Vascular Gasket. ACS Appl. Mater. Interfaces 2013, 5, 3757−3763.

(21) Jiang, J.; Li, Z. R.; Wang, H. J.; Carlson, M. A.; Teusink, M. J.; MacEwan, M. R.; Gu, L. X.; Xie, J. W. Cell Scaffolds: Expanded 3D Nanofiber Scaffolds: Cell Penetration, Neovascularization, and Host Response. Adv. Healthcare Mater. 2016, 5, 2993−3003.

(22) Jiang, J.; Carlson, M. A.; Teusink, M. J.; Wang, H. J.; MacEwan, M. R.; Xie, J. W. Expanding Two-Dimensional Electrospun Nanofiber Membranes in the Third Dimension By a Modified Gas-Foaming Technique. ACS Biomater. Sci. Eng. 2015, 1, 991−1001.

(23) Li, H. X.; Zhu, C. L.; Xue, J. J.; Ke, Q. F.; Xia, Y. N. Enhancing The Mechanical Properties of Electrospun Nanofiber Mats through Controllable Welding at The Cross Points. Macromol. Rapid Commun. 2017, 38, 1600723−1670023.

(24) Xue, J. J.; Yang, J. Y.; O'Connor, D. M.; Zhu, C. L.; Huo, D.; Boulis, N. M.; Xia, Y. N. Differentiation of Bone Marrow Stem Cells into Schwann Cells for the Promotion of Neurite Outgrowth on Electrospun Fibers. ACS Appl. Mater. Interfaces 2017, 9, 12299−12310.

(25) Liu, W. Y.; Lipner, J.; Moran, C. H.; Feng, L. Z.; Li, X. Y.; Thomopoulos, S.; Xia, Y. N. Generation of Electrospun Nanofibers with Controllable Degrees of Crimping through a Simple, Plasticizerbased Treatment. Adv. Mater. 2015, 27, 2583−2588. (26)

Lipner, J.; Shen, H.; Lenoardo, C.; Liu, W. Y.; Havlioqlu, N.; Xia, Y. N.; Galatz, L. M.; Thomopoulos, S. In Vivo Evaluation of Adipose-Derived Stromal Cells Delivered with a Nanofiber Scaffold for Tendon-to-Bone Repair. Tissue Eng., Part A 2015, 21, 2766−2774.

(27) Xie, J. W.; Liu, W. Y.; MacEwan, M. R.; Bridgman, P. C.; Xia, Y. N. Neurite Outgrowth on Electrospun Nanofibers with Uniaxial Alignment: The Effects of Fiber Density, Surface Coating, and Supporting Substrate. ACS Nano 2014, 8, 1878−1885.

(28) Jin, L.; Xu, Q. W.; Li, C.; Huang, J. B.; Zhang, Y. L.; Wu, D. C.; Wang, Z. L. Engineering 3D Aligned Nanofibers for Regulation of Cell Growth Behavior. Macromol. Mater. Eng. 2017, 302, 1600448− 1600448.

(29) Chen, X. X.; Han, M. D.; Chen, H. T.; Cheng, X. L.; Song, Y.; Su, Z. M.; Jiang, Y. G.; Zhang, H. X. A Wave-Shaped Hybrid Piezoelectric and Triboelectric Nanogenerator Nased on P(VDFTrFE) Nanofibers. Nanoscale 2017, 9, 1263−1270. (30) Jin, L.; Wu, D. C.; Kuddannaya, S.; Zhang, Y. L.; Wang, Z. L. Fabrication, Characterization, and Biocompatibility of Polymer Cored Reduced Graphene Oxide Nanofibers. ACS Appl. Mater. Interfaces 2016, 8, 5170−5177.

(31) Yuan, H. H.; Qin, J. B.; Xie, J.; Li, B. Y.; Yu, Z. P.; Peng, Z. Y.; Yi, B. C.; Lou, X. X.; Lu, X. W.; Zhang, Y. Z. Highly Aligned CoreShell Structured Nanofibers for Promoting Phenotypic Expression of vSMCs for Vascular Regeneration. Nanoscale 2016, 8, 16307−16322.

(32) Kratochvil, M. J.; Carter, M. C. D.; Lynn, D. M. Amine-Reactive Azlactone-Containing Nanofibers for the Immobilization and Patterning of New Functionality on

Nanofiber- Based Scaffolds. ACS Appl. Mater. Interfaces 2017, 9, 10243−10253.

(33) Ghasemi Hamidabadi, H.; Rezvani, Z.; Bojnordi, M. N.; Shirinzadeh, H.; Seifalian, A. M.; Jogahataei, T.; Razaghpour, M.; Alibakhshi, A.; Yazdanpanah, Y.; Salimi, M.; Mozafari, M.; Urbanska, A. M.; Reis, R. L.; Kundu; Gholipourmalekabadi, M. ChitosanIntercalated Montmorillonite/Poly(vinyl alcohol) Nanofibers as a Platform to Guide Neuronlike Differentiation of Human Dental Pulp Stem Cells. ACS Appl. Mater. Interfaces 2017, 9, 11392−11404.

(34) Xu, T.; Yang, H. Y. D.; Yang, Z.; Yu, Z. Z. Polylactic Acid Nanofiber Scaffold Decorated with Chitosan Islandlike Topography for Bone Tissue Engineering. ACS Appl. Mater. Interfaces 2017, 9, 21094−21104.

(35) Liu, X. H.; Jin, X. B.; Ma, P. X. Nanofibrous Hollow Microspheres Self-Assembled from Star-Shaped Polymers as Injectable Cell Carriers for Knee Repair. Nat. Mater. 2011, 10, 398−406.

(36) Baker, B. M.; Trappmann, B.; Wang, W. Y.; Sakar, M. S.; Kim, I. S.; Shenoy, V. B.; Burdick, J. A.; Chen, C. S. Cell-mediated Fibre Recruitment Drives Extracellular Matrix Mechanosensing in Engineered Fibrillar Microenvironments. Nat. Mater. 2015, 14, 1262− 1268.

(37) Hsiao, Y. S.; Liao, Y. H.; Chen, H. L.; Chen, P. L.; Chen, F. C. Organic Photovoltaics and Bioelectrodes Providing Electrical Stimulation for PC12 Cell Differentiation and Neurite Outgrowth. ACS Appl. Mater. Interfaces 2016, 8, 9275−9284.

(38) Guo, W. B.; Zhang, X. D.; Yu, X.; Wang, S.; Qiu, J. C.; Tang, W.; Li, L. L.; Liu,

H.; Wang, Z. L. Self-Powered Electrical Stimulation for Enhancing Neural Differentiation of Mesenchymal Stem Cells on GraphenePoly(3,4-ethylenedioxythiophene) Hybrid Microfibers. ACS Nano 2016, 10, 5086−5095.

(39) Yan, L.; Zhao, B. X.; Liu, X. H.; Li, X.; Zeng, C.; Shi, H. Y.; Xu, X. X.; Lin, T.; Dai, L. M.; Liu, Y. Aligned Nanofibers from Polypyrrole/Graphene as Electrodes for Regeneration of Optic Nerve via Electrical Stimulation. ACS Appl. Mater. Interfaces 2016, 8, 6834−3840.

(40) Jin, L.; Zeng, Z. P.; Kuddannaya, S.; Wu, D. C.; Zhang, Y. L.; Wang, Z. L. Biocompatible, Free-standing Film composed of Bacterial Cellulose Nanofibers/Graphene Composite. ACS Appl. Mater. Interfaces 2016, 8, 1011−1018.

(41) Cheng, J.; Jun, Y.; Qin, J. H.; Lee, S. H. Electrospinning Versus Microfluidic Spinning of Functional Fibers for Biomedical Applications. Biomaterials 2017, 114, 121−143.

(42) Yang, X.; Wei, J. H.; Lei, D. L.; Liu, Y. P.; Wu, W. Appropriate Density of PCL Nano-Fiber Sheath Promoted Muscular Remodeling of PGS/PCL Grafts in Arterial Circulation. Biomaterials 2016, 88, 34− 47.

(43) Murphy, A. R.; Laslett, A.; O'Brien, C. M.; Cameron, N. R. Scaffolds for 3D in Vivo Culture of Neural Lineage Cells. Acta Biomater. 2017, 54, 1−20.

(44) Zhang, K. H.; Zheng, H. H.; Liang, S.; Gao, C. Y. Aligned PLLA Nanofibrous Scaffolds Coated withGraphene Oxide for Promoting Neural Cell Growth. Acta Biomater. 2016, 37, 131−142.

(45) Hu, N.; Chang, H.; Zhang, H.; Wang, J.; Lei, W. X.; Li, B. C.; Ren, K. F.; Ji, J.

Mechanical Adaptability of the MMP-Responsive FilmImproves the Functionality of Endothelial Cell Monolayer. Adv. Healthcare Mater. 2017, 6, 1601410.

(46) Jin, L.; Xu, Q. W.; Kuddannaya, S.; Li, C.; Zhang, Y. L.; Wang, Z. L. Fabrication and Characterization of Three-Dimensional (3D) Core-Shell Structure Nanofibers Designed for 3D Dynamic Cell Culture. ACS Appl. Mater. Interfaces 2017, 9, 17718.

(47) Ma, Z. W.; Kotaki, M.; Yong, T.; Ramakrishna, S. Surface Engineering of Electrospun Polyethylene Terephthalate (PET) Nanofibers towards Development of A New Material for Blood Vessel Engineering. Biomaterials 2005, 26, 2527−2536.

(48) Landau, S.; Szklanny, A. A.; Yeo, G. C.; Shandalov, Y. L.; Kosobrodova, E.; Weiss, A. S.; Levenherg, S. Tropoelastin Coated PLLA-PLGA Scaffolds Promote Vascular Network Formation. Biomaterials 2017, 122, 72−82.

(49) Jin, L.; Zeng, Z. P.; Kuddannaya, S.; Yue, D.; Bao, J. N.; Wang, Z. L.; Zhang, Y. L. Synergistic Effects of A Novel Free-Standing Reduced Graphene Oxide Film and Surface Coating Fibronectin on Morphology, Adhesion and Proliferation of Mesenchymal Stem Cell. J. Mater. Chem. B 2015, 3, 4338−4344.

(50) Jin, L.; Feng, Z. Q.; Wang, T.; Ren, Z. Z.; Ma, S. S.; Wu, J. H.; Sun, D. P. A Novel Fluffy Hydroxylapatite Fibers Scaffold with Deep Interconnected Pores Designed for Three-Dimensional Cells Culture. J. Mater. Chem. B 2014, 2, 129−136. (51) Wu, S. Y.; Wang, J. D.; Jin, L.; Li, Y.; Wang, Z. L. Effect of Polyaryonitrile/MoS2 Composite Nanofibers on the Growth Behaviour of Bone Marrow Mesenchymal Stem Cells. ACS Appl. Nano Mater. 2018, 1, 337−343.

(52) Yan, L.; Xiang, Y.; Yu, J.; Wang, Y. B.; Cui, W. G. Fabrication of Antibacterial and

Antiwear Hydroxyapatite Coating via In Situ Chitosan-Mediated Pulse Electrochemical Deposition. ACS Appl. Mater. Interfaces 2017, 9, 5023−5030.

(53) Jin, L.; Yue, D.; Xu, Z. W.; Liang, G. B.; Zhang, Y. L.; Wang, Z. L. Fabrication, Mechanical Properties, and Biocompatibility of Reduced Graphene Oxide-Reinforced Nanofiber Mats. RSC Adv. 2014, 4, 35035−35041.

(54) Feng, Z. Q.; Wang, T.; Zhao, B.; Li, J. C.; Jin, L. Soft Graphene nanofibers designed for acceleration of nerve growth and development. Adv. Mater. 2015, 27, 6462−6468.